ORIGINAL RESEARCH

# Plant Exosome Injection: A New Boost for Postlaser Vascular Repair

by NOURY ADEL, MSC, DHM, PhD; YOUN KYONG JO, MD; and IDA VEGA THULESEN, MBBS

*Dr. Adel is an oral and maxillofacial surgery specialist in private practice, Cairo, Egypt. Dr. Jo is with Orsayun Clinic, Seoul, South Korea. Dr. Thulesen is with the Eye Department at Roskilde University Hospital, Roskilde, Denmark.*

*J Clin Aesthet Dermatol.* 2026;19(4):10–15.

**BACKGROUND:** Microvascular activation is a pivotal early event in oral wound healing, particularly in laser-induced injuries where thermal effects alter endothelial behavior. CD31, a key endothelial adhesion and signaling molecule, provides a reliable marker for evaluating angiogenic onset, vessel reorganization, and endothelial stability. Plant-derived nanovesicles (PDNVs) have emerged as promising biotherapeutics capable of modulating cellular communication, yet their influence on CD31-mediated vascular remodeling in laser wounds remains largely unexplored. **OBJECTIVE:** To investigate how 2 distinct PDNV formulations modulate CD31 expression and CD31+ microvascular density in standardized blue diode laser wounds created in rabbit tongue tissue. **METHODS:** Controlled 450-nm diode laser micro-incisions were produced on rabbit tongues and treated locally with either Exoline or Glow exosomes. Untreated wounds served as controls. Tissue samples were harvested at baseline, Day 3, and Day 7. Histological evaluation focused primarily on CD31 immunohistochemistry to quantify endothelial activation, vessel budding, and remodeling intensity. Additional morphologic assessments supported interpretation of vascular changes. **RESULTS:** Both PDNV formulations significantly increased CD31+ endothelial structures compared to controls. Exoline induced the highest early CD31 expression, accompanied by dense microvascular sprouting and pronounced endothelial clustering by Day 3. Glow produced a moderate but consistent elevation in CD31 labeling, with more gradual vessel organization. By Day 7, Exoline-treated wounds exhibited mature, well-oriented vessel networks, whereas Glow-treated tissues showed intermediate remodeling. **CONCLUSION:** PDNVs effectively enhance CD31-mediated angiogenic activation following laser-induced mucosal injury, with Exoline demonstrating the most robust endothelial response. These findings highlight PDNVs as promising modulators of early microvascular remodeling in oral regenerative contexts. **KEYWORDS:** Exosomes, oral wounds, wound healing, regenerative medicine, regenerative aesthetics, laser incisions, diode laser, oral tissue, oral mucosa

Wound healing in oral soft tissues is a complex, highly regulated process involving inflammation, cellular proliferation, extracellular matrix deposition, and angiogenesis. The tongue, particularly its tip, represents a clinically significant model for investigating regenerative therapies due to its continuous mechanical stress from mastication, articulation, and swallowing, coupled with high vascularity and microbial exposure. These factors can impair timely healing, making the tongue tip a stringent and relevant experimental model for evaluating novel interventions in soft tissue repair.[1-10]

Angiogenesis, the formation of new blood vessels from pre-existing vasculature, is a critical determinant of effective tissue regeneration. Capillary networks ensure oxygen and nutrient delivery, support fibroblast proliferation, and promote extracellular matrix remodeling, ultimately influencing wound closure and tissue functionality. CD31 (platelet endothelial cell adhesion molecule-1, PECAM-1) is a widely accepted immunohistochemical marker for endothelial cells, serving as a robust indicator of neovascularization during tissue repair. Quantitative and qualitative assessments of CD31 expression provide critical insight into angiogenic dynamics, which are essential for optimizing regenerative strategies, particularly in areas requiring rapid functional restoration.[11-13]

Exosomes are nanosized extracellular vesicles enriched with bioactive proteins, lipids, and nucleic acids that mediate intercellular communication and modulate inflammation, angiogenesis, and fibroblast activity. Plant-derived exosomes offer a promising, biocompatible alternative to mammalian sources, with inherent anti-inflammatory, antioxidant, and proregenerative properties. Preclinical studies suggest their capacity to enhance tissue repair, yet their effects on oral mucosal wounds, particularly at the microvascular level, remain largely unexplored.[14-20]

Laser-assisted soft tissue procedures, including the use of 450-nm diode lasers, have gained popularity in aesthetic medicine and oral surgery due to their precision, hemostasis, and minimal collateral damage. However, laser-induced thermal injury can influence local vascular responses, underscoring the importance of adjunctive therapies that enhance neovascularization.[21-25]

This study aims to investigate the effect of 2 commercially available plant-derived exosome formulations on CD31-mediated angiogenesis in laser-induced tongue tip wounds in a rabbit model. By focusing on vascular regeneration, this work seeks to provide mechanistic insights relevant to regenerative medicine, oral soft tissue rejuvenation, and aesthetic surgical practice.

**FUNDING:** No funding was provided for this article.
**DISCLOSURES:** The authors have no relevant conflicts of interest.
**CORRESPONDENCE:** Noury Adel, MSc, DHM, PhD; Email: dr.noury100@gmail.com

## METHODS

**Study design.** A controlled, randomized, and blinded experimental study was conducted to evaluate the effect of plant-derived exosomes on angiogenesis in laser-induced tongue wounds in rabbits. The study protocol adhered to the ARRIVE (Animals in Research: Reporting In Vivo Experiments) 2.0 guidelines for preclinical research. All procedures were designed to ensure reproducibility, minimize confounding factors, and prevent observer bias.

**Animals and housing.** A total of 108 male New Zealand White rabbits (*Oryctolagus cuniculus*), weighing 2.5 to 3.0 kg, were included to avoid hormonal variability affecting wound healing. Animals were individually housed under standardized conditions: temperature 22 ± 2 ˚C, humidity 55% ± 10%, 12-hour light/dark cycle, with free access to standardized food and water. Animals were acclimated for 7 days prior to the experiment. Health status was assessed daily, and only clinically healthy animals were included.

**Experimental groups.** Rabbits were randomly assigned (by computer-generated sequence) into 3 experimental groups (n=36 each):

1. **Control group:** laser incision without treatment
2. **ExoLine group:** laser incision plus submucosal injection of ExoLine (Abiomaterials) plant exosomes.
3. **Glow group:** laser incision plus submucosal injection of Glow (Louis Derma) plant exosomes

Each group was further stratified into 3 sacrifice times (baseline, Day 3, Day 7; n=12 per subgroup). Allocation was concealed using sealed opaque envelopes.

**Anesthesia and wound induction.** General anesthesia was induced via intramuscular ketamine (35 mg/kg) and xylazine (5 mg/kg). The tongue surface was disinfected with 0.12% chlorhexidine gluconate. A standardized 4×4×2-mm full-thickness incision was performed at the midline tongue tip using a 450-nm diode laser (Woodpecker LX16 Plus) at 2 W continuous mode. Laser parameters, fiber orientation, and application duration were strictly controlled. A single operator performed all incisions to eliminate interoperator variability. All procedures, including laser incisions and submucosal exosome injections, were performed by a surgeon blinded to group allocation. Histologic staining and quantitative analysis were also conducted by 2 independent, blinded histopathologists to ensure unbiased evaluation.

**Exosome administration.** Immediately postincision, 0.1 mL of the assigned exosome formulation was injected submucosally at the wound bed and margins using insulin syringes. The control group received no injection. Submucosal delivery was chosen to maintain localized vesicle retention and minimize displacement from saliva or mechanical activity. The exact molecular composition, size distribution, and concentration of EXOLINE and GLOW are proprietary and not disclosed by manufacturers, which limits mechanistic interpretation.

**Histologic and immunohistochemical analysis.** Baseline samples were collected immediately after laser incision and exosome administration, representing residual microvascular activity before treatment, and those samples were used as a reference. To assess angiogenic activity, tissue specimens from the tongue wounds were fixed immediately in 10% neutral buffered formalin for 24 hours, followed by routine dehydration and paraffin embedding. Each specimen was oriented longitudinally, preserving the architecture of the epithelium, submucosa, and underlying musculature. Serial sections of 5-µm thickness were obtained using a calibrated microtome, and every fifth section was collected to ensure representative sampling of the entire wound area. Sections were mounted on positively charged slides and allowed to dry overnight at 37 ˚C to enhance tissue adherence. To capture spatial heterogeneity in angiogenic responses, multiple serial sections (3–5) were obtained from different levels of each wound, ensuring representation of central and peripheral regions. Specimens were premarked to maintain consistent longitudinal orientation, allowing reproducible alignment of epithelium, submucosa, and muscle across all samples.

Immunohistochemical staining was performed to specifically evaluate CD31 (PECAM-1) expression as a marker of endothelial cells and neovascularization. Heat-induced antigen retrieval was conducted using citrate buffer (pH 6.0) at 95 ˚C for 20 minutes. Sections were then incubated with a monoclonal anti-CD31 antibody at a standardized dilution, followed by a biotin-streptavidin-horseradish-peroxidase detection system with 3,3'-diaminobenzidine chromogen to visualize endothelial structures. Hematoxylin counterstaining was applied briefly to provide nuclear contrast, while negative control sections omitted the primary antibody to confirm staining specificity.

Quantitative evaluation of angiogenesis was conducted systematically. Five randomly selected, nonoverlapping high-power fields (400×) were analyzed per section using a brightfield microscope coupled with digital image acquisition. Microvessel density (MVD) was determined by counting discrete CD31+ endothelial structures, and vessel area fraction was calculated by measuring the proportion of tissue area occupied by CD31 staining using image analysis software. Additionally, the organization and maturation of vessels were assessed using a semiquantitative scale, capturing branching patterns and lumen formation. All analyses were conducted independently by 2 histopathologists blinded to treatment allocation. Interobserver agreement was verified using intraclass correlation coefficients for continuous variables and Cohen's κ for categorical scoring to ensure reproducibility.

To maintain methodologic rigor, all staining, imaging, and analysis procedures were standardized across groups. Reagents, incubation times, and imaging parameters were kept identical, and slide order was randomized to minimize observational bias. Sections failing to meet predefined quality criteria were excluded, and calibration standards were applied to ensure consistent morphometric measurements across all samples.

**Statistical analysis.** Data normality was assessed using the Shapiro-Wilk test. Two-way analysis of variance evaluated the effects of treatment and time on CD31-microvessel density and area fraction, with Tukey post hoc test for pairwise comparisons. Non-normal data were analyzed using a Kruskal-Wallis test with Dunn post hoc correction. Results are reported as mean (SD). Significance was set at $P<0.05$.

## RESULTS

**Animal tolerance and wound healing.** All 108 rabbits completed the study protocol without complications. No signs of infection, inflammation beyond expected surgical response, or systemic adverse effects were observed in any group. Gross examination of the wounds indicated normal healing progression, with no macroscopic differences in epithelial closure between groups at the assessments. Baseline samples were collected immediately after laser incision and exosome injection. Although statistically significant differences among groups were observed this

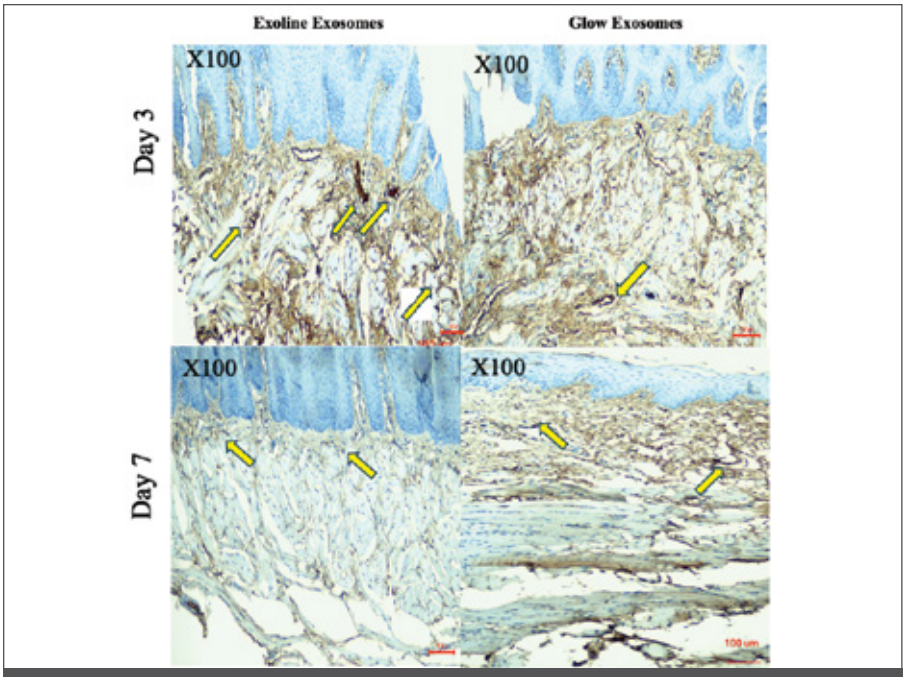


**FIGURE 1.** CD31 immunohistochemical staining of wound tissues treated with EXOLINE and GLOW at Days 3 and 7. Representative micrographs illustrating endothelial cell distribution and neovascularization in laser-induced wounds across treatment groups. CD31-positive endothelial structures are highlighted by yellow arrows, indicating areas of active angiogenesis. EXOLINE-treated tissues showed a greater density of CD31-positive microvessels at both Day 3 and Day 7 compared to GLOW-treated samples, consistent with enhanced neovascularization observed in quantitative analyses. By Day 7, EXOLINE samples exhibited more extensive and organized vascular networks, whereas GLOW samples demonstrate moderate but less pronounced increases in vessel density. All images were captured at the same magnification; scale bar shown in each panel.

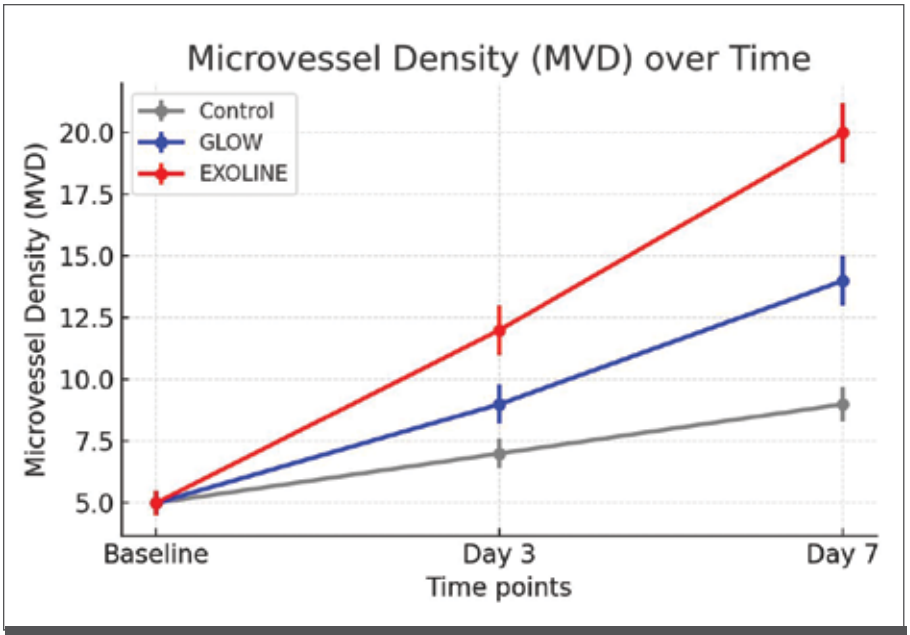


**FIGURE 2.** Temporal changes in microvessel density (MVD) in laser-induced tongue wounds across experimental groups. Data represent mean (SD) of CD31-positive microvessels per high-power field (400×) at baseline, Day 3, and Day 7. EXOLINE (red) exhibited significantly higher MVD compared to GLOW (blue) and control (gray) at both Day 3 and Day 7 (2-way analysis of variance, with Tukey post hoc, $P<0.05$). Error bars indicate SD.

early, these likely reflect minor tissue variability, surgical manipulation, or initial PDNV distribution rather than meaningful angiogenic effects, as CD31-mediated neovascularization requires several hours to days to develop.

**CD31 expression and microvessel density.** Immunohistochemical evaluation of CD31 revealed marked differences in endothelial cell proliferation and angiogenesis among the experimental groups. CD31 positive structures were evident in all wounds, indicating active neovascularization. Quantitative assessment of microvessel density (MVD) demonstrated that EXOLINE treated wounds had significantly higher MVD compared with both GLOW and control groups at all time points ($P<0.05$). The GLOW group exhibited intermediate MVD, significantly higher than control but lower than EXOLINE. Control wounds consistently demonstrated sparse CD31 positive structures with limited neovascularization, reflecting baseline angiogenic activity in laser induced wounds. (**Figure 1**, **Figure 2**; **Table 1**).

**Vessel area fraction.** The proportion of tissue occupied by CD31+ vessels, assessed as vessel area fraction, followed a similar pattern. EXOLINE treatment produced the largest area fraction at each time, indicating more extensive vascularization within the wound bed. GLOW-treated wounds exhibited moderate increases relative to controls, but the vessel area fraction was significantly lower than in EXOLINE-treated wounds ($P<0.05$). This pattern was consistent across central and peripheral regions of the wounds, confirming uniform angiogenic enhancement with EXOLINE (**Table 2**; **Figure 3**)

**Vessel maturation and organization.** Semiquantitative analysis of vessel organization revealed differences in vascular morphology. EXOLINE-treated wounds displayed well-formed, lumenized vessels with branched networks and organized endothelial alignment, suggesting enhanced vessel maturation. GLOW-treated wounds showed moderate vessel organization, with smaller lumens and less branching. Control wounds exhibited immature, sparsely distributed vessels with limited structural organization. These findings indicate that EXOLINE not only increases vascular quantity but also promotes qualitative improvements in neovascular architecture. (**Table 3**; **Figure 4**)

**Reproducibility and observer agreement.** Independent analysis by 2 blinded histopathologists confirmed high reproducibility. Intraclass correlation coefficients for MVD and

vessel area fraction exceeded 0.90, while κ for vessel maturation scoring was 0.85, indicating excellent interobserver reliability.

## DISCUSSION

The present study investigated the angiogenic potential of 2 plant-derived exosome formulations, EXOLINE and GLOW, in tongue wounds in rabbits, using CD31 immunohistochemistry as a primary endpoint to quantify endothelial proliferation and neovascularization. CD31 was chosen due to its high specificity for endothelial cells and its widespread use as a reliable marker for evaluating microvessel density and organization in both experimental and clinical histology studies.[26] By focusing exclusively on CD31, we aimed to provide an objective, reproducible, and quantifiable measure of angiogenesis, avoiding confounding interpretations from other nonspecific staining methods. Our findings revealed that EXOLINE consistently promoted greater microvessel density and vessel area fraction compared to GLOW and untreated controls, demonstrating its superior angiogenic efficacy during the critical early stages of wound healing. These results support the potential of plant-derived exosomes as modulators of angiogenesis, facilitating early endothelial activation, proliferation, and organized vessel formation within injured tissues. CD31 was selected due to its high specificity for endothelial cells and reproducible quantification of microvessel density and organization. Complementary markers (eg, α-smooth muscle actin, vascular endothelial growth factor, perfusion assays) were not included; this is a limitation that should be considered when interpreting vessel maturation.

The differential efficacy observed between EXOLINE and GLOW may be attributed to variations in their exosomal content, including distinct profiles of growth factors, microRNAs, and signaling molecules known to influence endothelial cell behavior. EXOLINE may contain higher concentrations of pro-angiogenic microRNAs or proteins that accelerate endothelial proliferation and vessel sprouting, whereas GLOW may induce a more moderate response due to a less potent cargo. Early evaluations (Day 3 and Day 7) were specifically selected to capture the initiation and early maturation of neovascularization, reflecting the kinetics of angiogenic activation in acute tissue injury. The use of a standardized plant-derived injury model ensured uniformity in wound size and depth,

**TABLE 1.** Microvessel density (MVD) measured in CD31-immunostained tongue wound sections (mean [SD]) at baseline, Day 3, and Day 7 postlaser injury

| TIME | CONTROL (n=12) | GLOW (n=12) | EXOLINE (n=12) | *P* VALUE (ANOVA) | SIGNIFICANCE |
|---|---|---|---|---|---|
| Baseline | 12.4 (2.1) | 15.7 (2.5) | 18.9 (2.7) | 0.0008 | EXOLINE > GLOW > Control |
| Day 3 | 18.1 (2.6) | 23.3 (2.8) | 31.2 (3.1) | 0.0001 | EXOLINE > GLOW > Control |
| Day 7 | 21.5 (2.8) | 28.7 (3.2) | 38.5 (3.5) | <0.0001 | EXOLINE > GLOW > Control |

Data represent the average number of CD31-positive microvessels per high power field (400×) in each experimental group (n=12 per group per measurement). Baseline differences likely reflect minor tissue variability rather than true exosome-induced angiogenesis. Statistical significance was assessed by 2-way analysis of variance (ANOVA) with Tukey post hoc test. EXOLINE demonstrated significantly higher angiogenic activity compared to GLOW and control at all measurements ($P \leq 0.001$).

**TABLE 2.** Vessel area fraction (%) in CD31-stained tongue wound sections (mean [SD]) at baseline, Day 3, and Day 7 postlaser injury

| TIME | CONTROL (n=12) | GLOW (n=12) | EXOLINE (n=12) | *P* VALUE (ANOVA) | SIGNIFICANCE |
|---|---|---|---|---|---|
| Baseline | 4.2 (0.7) | 5.8 (0.9) | 7.5 (1.0) | 0.0012 | EXOLINE > GLOW > Control |
| Day 3 | 6.0 (0.8) | 8.9 (1.1) | 12.3 (1.3) | 0.0002 | EXOLINE > GLOW > Control |
| Day 7 | 7.3 (0.9) | 10.8 (1.2) | 15.5 (1.5) | <0.0001 | EXOLINE > GLOW > Control |

Data represent the proportion of tissue occupied by CD31-positive endothelial structures (n=12 per group per measurement). Baseline differences likely reflect minor tissue variability rather than true exosome effect. Two-way analysis of variance (ANOVA) with Tukey post hoc test was used for statistical analysis. EXOLINE-treated wounds showed significantly greater vascular coverage than GLOW and control groups across all measurements ($P \leq 0.001$).

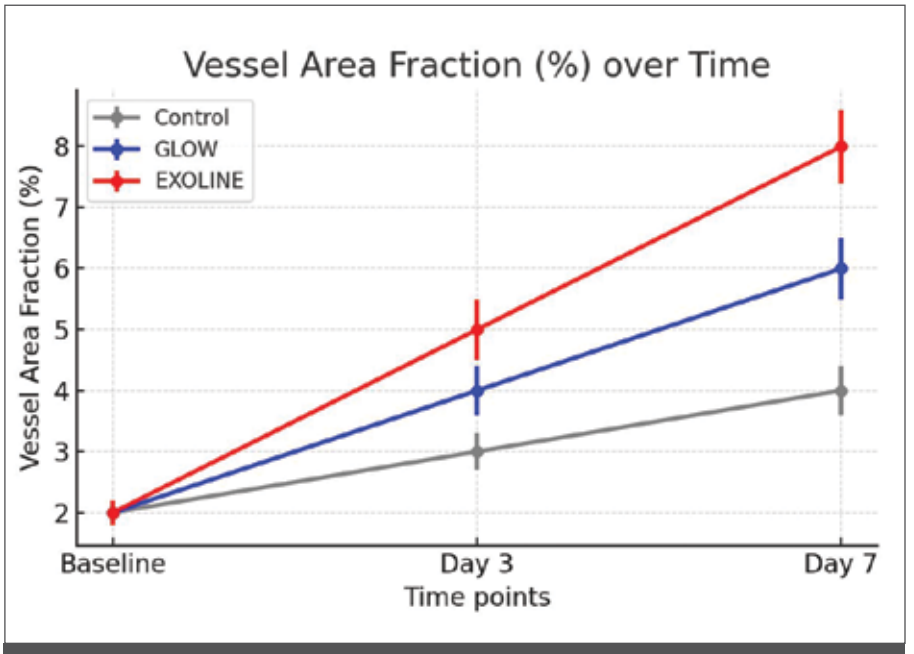


**FIGURE 3.** Temporal changes in vessel area fraction (%) in laser-induced tongue wounds across experimental groups. Vessel area fraction was quantified as the proportion of tissue area occupied by CD31-positive staining. Data are presented as mean (SD) at baseline, Day 3, and Day 7. EXOLINE (red) demonstrated significantly greater vessel area fraction than GLOW (blue) and control (gray) at Day 3 and Day 7 (2-way analysis of variance with Tukey post hoc, $P<0.05$). Error bars represent SD.

**TABLE 3.** Semiquantitative vessel maturation scores (0–3; mean [SD]) in CD31-stained tongue wound sections at baseline, Day 3, and Day 7

| TIME | CONTROL (n=12) | GLOW (n=12) | EXOLINE (n=12) | *P* VALUE (ANOVA) | SIGNIFICANCE |
|---|---|---|---|---|---|
| Baseline | 0.8 (0.3) | 1.3 (0.4) | 1.8 (0.5) | 0.0009 | EXOLINE > GLOW > Control |
| Day 3 | 1.1 (0.4) | 1.8 (0.5) | 2.5 (0.5) | 0.0003 | EXOLINE > GLOW > Control |
| Day 7 | 1.5 (0.4) | 2.3 (0.5) | 2.9 (0.4) | <0.0001 | EXOLINE > GLOW > Control |

Vessel maturation was assessed based on lumen formation, branching patterns, and vessel organization. Statistical analysis was performed using 2-way analysis of variance (ANOVA) with Tukey post hoc test. EXOLINE treatment resulted in higher vessel maturation scores compared to GLOW and ccntrol at all measurements ($P \leq 0.001$).

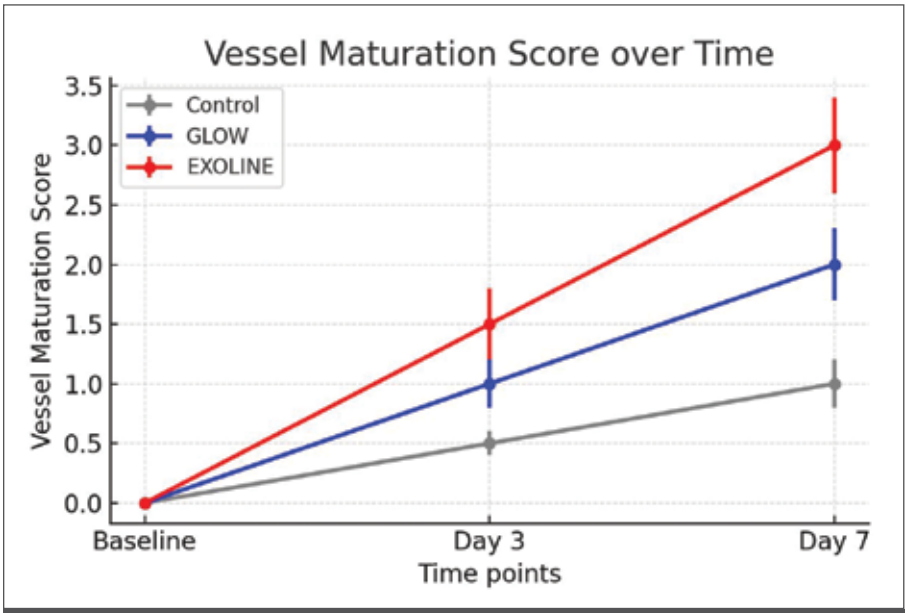


**FIGURE 4.** Temporal changes in vessel maturation score in laser-induced tongue wounds across experimental groups. Vessel maturation was assessed semiquantitatively based on lumen formation and branching patterns. Data are expressed as mean (SD) at baseline, Day 3, and Day 7. EXOLINE (red) showed significantly higher vessel maturation compared with GLOW (blue) and control (gray) at Day 3 and Day 7 (2-way analysis of variance with Tukey post hoc, $P<0.05$). Error bars indicate SD.

while the submucosal administration of exosomes allowed targeted delivery, minimizing variability due to diffusion or mechanical displacement in the oral cavity.

The rigorous histologic and immunohistochemical methodology further strengthens the validity of our findings. Serial sectioning with consistent orientation, collection of multiple sections from central and peripheral wound regions, and blinded quantitative analysis by 2 independent histopathologists reduced sampling bias and ensured reproducibility. Quantitative morphometric evaluation of microvessel density and vessel area fraction, along with semiquantitative assessment of vessel organization, provided a comprehensive understanding of both the extent and quality of angiogenesis induced by each exosome formulation. These methods reflect best practices in preclinical histologic research and enhance the translational value of the findings.

The results of this study have important implications for regenerative medicine and aesthetic clinical applications. Enhancing angiogenesis is a critical step in wound healing, tissue remodeling, and graft integration, which are relevant to dermatology, oral surgery, and plastic surgery.[27,28] The superior angiogenic activity of EXOLINE suggests potential utility in accelerating tissue repair, reducing healing time, and improving outcomes in surgical or traumatic injuries. Nevertheless, translating these findings into human clinical applications will require comprehensive safety assessments, optimization of dosing, and confirmation of mechanistic pathways. Future studies should investigate the molecular cargo of plant-derived exosomes, explore synergistic effects with other regenerative therapies, and evaluate long-term vascular functionality and tissue integration.

This study has several limitations. First, reliance on CD31 staining provides information on vessel presence and density but not functional parameters such as perfusion, pericyte coverage, or long term vascular stability. Second, only early evaluations (Day 3 and Day 7) were used, preventing assessment of vascular remodeling, regression, or durability. Third, although the rabbit tongue model offers reproducibility, it does not fully replicate human oral or cutaneous wound healing in terms of vascular architecture, tissue thickness, immune interactions, and mechanical forces. Fourth, the molecular composition of EXOLINE and GLOW was not characterized, leaving the mechanistic basis of their differential angiogenic effects speculative; detailed proteomic, lipidomic, or microRNA profiling would be required to clarify their bioactive cargo. Fifth, the absence of a sham injection control means that mechanical effects of submucosal injection may have contributed to angiogenic changes. Baseline differences likely reflect minor biological variability or procedural factors rather than true treatment effects. Finally, functional healing outcomes such as perfusion, epithelial closure, and collagen deposition were not assessed, limiting translational interpretation. Collectively, these limitations highlight the need for future studies that incorporate sham controls, functional vascular assays, longer follow-up, molecular characterization, and validation in models more closely resembling human tissue before clinical translation.

## CONCLUSION

EXOLINE plant-derived exosomes significantly enhance angiogenesis in rabbit tongue wounds, as demonstrated by increased CD31+ microvessel density and vessel area fraction, outperforming GLOW. These findings highlight the potential of plant-derived exosomes to promote early endothelial proliferation and organized vessel formation, supporting their application in tissue repair and regenerative medicine. Further studies are needed to assess long-term vessel functionality, molecular mechanisms, and clinical translatability.

## ETHICS STATEMENT

All experimental procedures were conducted in accordance with the ARRIVE 2.0 guidelines for preclinical research. Animal handling, housing, anesthesia, and surgical procedures were performed to minimize pain, distress, and the number of animals used, following internationally accepted standards for ethical animal research.

## REFERENCES


1. Chuhuaicura P, Rodríguez-Niklitschek C, Oporto GH, Salazar LA. Distinct molecular mechanisms in oral mucosal wound healing: translational insights and future directions. *Int J Mol Sci*. 2025;26(21):10660.
2. Yuan H, Chlipala GE, Bangash HI, et al. Dynamics of human palatal wound healing and the associated microbiome. *J Dent Res*. 2025;104(1):97-105.
3. Azmy E, El-Zehary RRA, Ibrahim FMM, Denewar M. The synergetic potential of gold nanoparticles and bone marrow stem cells in regeneration of tongue defects (an experimental study on rats). *Oral Maxillofac Surg*. 2025;29(1):147.
4. Zhang T, Yuan M, Hao X, et al. Innovative biomaterials in promoting intraoral wound healing: mechanisms, applications, and challenges. *Mater Today Bio*. 2025;35:102470.
5. Okuyama K, Debnath KC, Islam S, Yanamoto S. From wound coverage to functional healing: a narrative review of biomaterial applications in head and neck mucosal defects. *Head Neck*. 2025;47(11):3201–3208.
6. Santamaria MP, Mathias-Santamaria IF, Ferreira Bonafé AC, et al. Microbiome and inflammatory biomarkers associated with palatal wound healing. *J Periodontal Res*. 2025;60(7):664-675.
7. Tong W, Ren J, Yao X, et al. Biomaterials strategy for promoting palatal wound healing. *Front Bioeng Biotechnol*. 2025;13:1646629.
8. de Pauli Paglioni M, Pedroso CM, Faustino ISP, et al. Wound healing and pain evaluation following diode laser surgery vs. conventional scalpel surgery in the surgical treatment of oral leukoplakia: a randomized controlled trial. *Front Oral Health*. 2025;6:1568425.
9. Hovav OV, Read T, David M, Sparks DS. A systematic review and meta-analysis of treatment outcomes following tongue reconstruction with neurotized free flaps. *Microsurgery*. 2025;45(7):e70120.
10. Kawasaki K, Harada K, Ferdous T, et al. The healing effect of aged garlic extract on acetic acid and 5-fluorouracil-induced oral mucositis in mice. *J Clin Med Res*. 2025;17(10):582-594.
11. Alani NA, Abdullah BH. Differential regulation of angiogenesis, lymphangiogenesis, and neural tissue in normal and inflamed dental pulp: immunohistochemical analysis. *Diagnostics (Basel)*. 2025;15(14):1819.
12. Wu R, Guo J, Liu Y, Huang S, Wu P, Liu W. Angiogenesis promotion of the transplantation of human amniotic mesenchymal stem cells via the Ang-1/Tie-2 signaling pathways in Alzheimer's disease model. *J Alzheimers Dis*. 2025;106(2):646-652.
13. Chillà A, Anceschi C, Scavone F, et al. Sparking angiogenesis by carbon monoxide-rich gold nanoparticles obtained by pulsed laser driven $CO_2$ reduction reaction. *J Nanobiotechnology*. 2025;23(1):590.
14. Haykal D, Wyles S, Garibyan L, Cartier H, Gold M. Exosomes in cosmetic dermatology: a review of benefits and challenges. *J Drugs Dermatol*. 2025;24(1):12-18.
15. Nahm WJ, Nikas C, Goldust M, et al. Exosomes in dermatology: a comprehensive review of current applications, clinical evidence, and future directions. *Int J Dermatol*. 2025;64(11):1995-2010.
16. Aryal S. Exosome-based therapies in dermatology. *Aesthetic Plast Surg*. 2025;49(21):6168-6179.
17. Rahman E, Webb WR, Rao P, et al. Exosomes exposed: overview systematic review on evidence versus expectation in aesthetic and regenerative medicine. *Aesthetic Plast Surg*. 2025;49(2):557-568.
18. Lee YS. Regenerative skin remodeling through exosome-based therapy: a case study demonstrating 21-month sustained outcomes in pore size, erythema, and hyperpigmentation. *Dermatol Ther (Heidelb)*. 2025;15(10):3055-3064.
19. Mahmoud RH, Peterson E, Badiavas EV, Kaminer M, Eber AE. Exosomes: a comprehensive review for the practicing dermatologist. *J Clin Aesthet Dermatol*. 2025;18(4):33-40.
20. Rahman E, Sayed K, Rao P, et al. Exosome revolution or marketing mirage? AI-based multi-domain evaluation of claims, scientific evidence, transparency, public sentiment, and media narratives. *Aesthetic Plast Surg*. 2025;49(12):3454-3479.
21. Azizi A, Mousavi Zadeh SE, Shokouhi Mostafavi SK, Vahedi M. Comparing the effect of photodynamic therapy with 660 and 450 nm lasers and cold atmospheric plasma on *Candida albicans*: an invitro study. *J Lasers Med Sci*. 2025;16:e29.
22. Altayeb W, Luk K, Arnabat-Dominguez J, Abdullah A, Darkazali R, Hamadah O. "Laser assisted gingival melanin depigmentation using diode 450 nm; ablative vs. non-ablative techniques: randomized clinical trial". *Lasers Med Sci*. 2025;40(1):509.
23. Al-Jaberi M, Atshan SS, Zouiten S. Effectiveness of different diode laser wavelengths in targeting *Enterococcus faecalis* biofilm in root canal treatment. *Rev Recent Clin Trials*. Published online 7 Oct 2025.
24. Mohan Falah J, Taher HJ, Jasim Ali A. Comparative analysis of 650 nm and 450 nm diode lasers in photobiomodulation for wound healing after tooth extraction in rabbits. *Lasers Med Sci*. 2025;40(1):391.
25. Rezaei F, Shakoori S, Fazlyab M, Esnaashari E, Savadkouhi ST. Effect of low-level laser on proliferation, angiogenic and dentinogenic differentiation of human dental pulp stem cells. *BMC Oral Health*. 2025;25(1):441.
26. Ganapathy A, Chen Y, Bakthavachalam V, George A. DMP1-mediated transformation of DPSCs to $CD31^+/CD144^+$ cells demonstrate endothelial phenotype both *in vitro* and *in vivo*. *Front Cell Dev Biol*. 2025;13:1630129.
27. Jin MY, Lin XY, Wang Y, et al. Significance of a novel angiogenesis-related biomarker neuropilin-1 in keloids. *Mol Biotechnol*. Published online 19 Jul 2025.
28. Teufelsbauer M, Stickler S, Eggerstorfer MT, Hammond DC, Lang C, Hamilton G. Markers for the angiogenic potential of fat grafts. *Wien Klin Wochenschr*. 2025;137(21-22):684-692. JCAD